WILEY *fib*

TECHNICAL PAPER

Determination of volume and distribution of pores of concretes according to different exposure classes through 3D microtomography and mercury intrusion porosimetry

Fernanda Pacheco[1] | Rodrigo Périco de Souza[1] | Roberto Christ[1] | Clarissa Argenti Rocha[1] | Luis Silva[2] | Bernardo Tutikian[1] (iD)

[1]Universidade do Vale do Rio dos Sinos, São Leopoldo, Brazil

[2]Universidad de la Costa, Barranquilla, Colombia

Correspondence
Bernardo Tutikian, Universidade do Vale do Rio dos Sinos, UNISINOS, Avenida Unisinos, no 950, CEP 93.022-750, São Leopoldo, RS, Brasil.
Email: bftutikian@unisinos.br

Diagnosing and understanding the properties of concrete structures allows its use in more effective ways that neither compromise application nor impose safety risks or waste materials. Several tests can be performed for this purpose, differing with regards to diagnostic precision, complexity of execution, costs, need of specific apparatus, and others. Specifications from standards must be followed to assure the durability of concrete structures, such as Eurocode 1 (EN 1992-1) and EN 206 in Europe. This study determined the volume and the distribution of pores of four concrete compositions with distinct water/cement ratio, cement consumption, and compressive strength, through tests of mercury intrusion porosimetry (MIP) and 3D microtomography. Results showed high correlation coefficients between the tests for assessing voids and compressive strength. Comparatively, the 3D microtomography test presented linear relation to the specifications of mixtures, although MIP indicated discrepancies for mixture 2.

KEYWORDS
3D microtomography, concrete durability, mercury intrusion porosimetry

1 | INTRODUCTION

The durability of structures is described as the period during which there is no loss of performance or functional capacity due to environmental characteristics.[1] According to Gjorv,[2] such aspect not only impacts the state of design of structures, but is also influenced by the quality of the concrete used on the structures, being a safeguard to its use.

Changes resulting from the development of cities led to more abundant deteriorations of structures, mainly due to the influx of carbon dioxide and chloride ions.[3] The diffusion of these agents within concretes depends of its composition characteristics established by national and international standards, taking into account the influence exerted by cement consumption, water/cement ratio and compressive strength and the durability of the structures (EN 1992-1).[4–8]

Considering the impact caused by buildings, whether through energy for producing inputs, the construction process itself or by extracting raw materials from nature, it is mandatory to evaluate the durability of buildings to achieve a relation between lifespan requirements and environmental impact of its outset.[9]

Structures design present limitations regarding to the structural components type and use of and environmental characteristics of their zones of insertion, in addition to constant weather condition changes.[10] And so, the specification of mixtures may be an inefficient way to ensure durability,

wileyonlinelibrary.com/journal/suco **1**

which in turn is related to compressive strength.[11] In fact, porosity and interconnectivity of concrete pores are indispensable characteristics certifiable through correct specification and composition of mixtures.[12] Some relations can be proposed, such as those that relate buildings' susceptibility to attack by carbon gas to their initial water absorption rate, which is directly influenced from the elements porosity.[13]

In terms of specification seeking durability, the need to correctly proportionate the mixtures although amount of water and reduction of porosity should be emphasized[14] Moreover, a cement adequate for chemically protecting reinforcements should be used, along with minimal fines content.[15]

These characteristics of composition can foresee durability and can be assessed though advanced diagnostic tests. Such analyses can be used for quality control of materials during production and development.

The mercury intrusion porosimetry (MIP) test was used before for comparing concrete compositions and correlating the compressive strength of such compositions.[16] The purpose of this method was to validate the pozzolans usage and measure their effect on the microstructure of the concretes.[17]

Imaging diagnostic tests also turn out to be an option for identifying distribution and quantity of pores with higher precision. The most commonly used for durability of concrete structures is the 3D microtomography, which has wide range of uses in materials science. It consists of a technique that verifies images of the sample's total volume sequentially.[18] Moreover, this technique has been used as a means to identify the formation of cracks on cementitious materials and correlate the results to the lifespan of the structure.[19]

Considering the need to understand properties of concrete through diagnostic tests, four concrete compositions were mixed under parameters set by Eurocode 1 (EN 1992-1) and EN 206-1, according to the aggressiveness of the environment that the structure is exposed to. The aim was to assess the relation between tests of MIP and 3D microtomography and the mechanical properties of the material.

2 | ADVANCED DIAGNOSTIC TESTS

2.1 | Mercury intrusion porosimetry

For this test, mercury is injected into a sample and its penetration is forced by applying pressures, which yield the volume of voids within the material. It is mainly a technique for diagnosing cementitious composites as it reveals porosity and the consequent susceptibility to attacks by deterioration agents.[20,21]

In this context, MIP was used for relating characteristics of concrete to results of accelerated carbonation tests, confirming the relation between porosity and fronts of aggression, which proved to be a coherent estimation of durability.[22] Water absorption tests also aimed to evaluate concretes produced in laboratory and at construction site, so these methods consisted of a way for approving the concrete used, guaranteeing the quality of the elements.[11] Another advantage is the test samples are smaller, allowing their use for lifespan analyses.

Concerning size of pores of concrete samples, it was found out that there is a relation between their diameter, measured by the porosimetry test, and the type of mass transportation that occurs inside the material, as the dimensions of these physical phenomena were identifiable.[23] Moreover, the phenomena of gaseous diffusion and ionic migration occur in pores with sizes between 10^{-2} and 10^{-9} m, whereas pores with size of 10^{-7} m or higher can allow permeability of concrete, and capillarity occurs in pores with sizes between 10^{-3} and 10^{-7} m.[24]

2.2 | 3D microtomography

The 3D microtomography technique is used for analyzing and diagnosing the microstructure of several materials although a series of images that devise the sample's volumetry, identifies its voids and aligns fibers, for materials of diverse densities. It is also possible to detect areas of pastes, dense and porous and voids between aggregates for cementitious materials.[25]

The graphical depiction of different components of a single matrix is made possible by analyzing the difference of density between its ingredients. Nonetheless, X-ray absorption, which differs from material to material, allows contrast to be seen and exposes its existence and distribution along the sample.[26]

An evaluation of cement pastes at different ages combining the techniques of 3D microtomography and scanning electron microscopy pointed out the presence of voids and anhydrous cement.[27] Such techniques were also used for assessing a matrix of advanced cementitious composites, whereas focusing on the interface between fibers and cement paste.[23] The procedure turned out to be appropriate for analyzing the transitioning zone between paste and fiber, pointing towards an adequate adherence with no void agglomerations. Finally, this procedure was put into use for measuring and analyzing the distribution of voids with respect to pore size of a fiber-reinforced concrete, resulting in a void diameter preponderantly between 0.39 and 0.77 mm.[28]

The technique can be applied for evaluating pore connectivity, thus allowing the understanding of its relation with characteristics such as water absorption and durability of the material.[29] An experimental procedure was then carried out comprising diagnostic tests on concretes specified in accordance with EN 1992-1 and EN 206 to validate conclusions drawn by other studies.

TABLE 1 Composition characteristics of mixtures

Mixture	Compressive strength (MPa)	Cement consumption (kg/m^3)	Water/cement ratio	Exposure
M1	25	260	0.65	Dry weather
M2	30	280	0.60	Water forces
M3	35	320	0.55	Salty fog
M4	40	360	0.45	Chemical aggression

TABLE 2 Particle-size distribution of aggregates

Sieve opening (mm)	Fine aggregate		Coarse aggregate	
	% Retained	% Retained accumulated	% Retained	% Retained accumulated
9.5	0	0	20	20
6.3	0	0	48	68
4.8	1	1	18	86
2.4	3	4	13	99
1.2	7	11	1	100
0.6	11	22	0	100
0.3	26	48	0	100
0.15	51	99	0	100
Bottom	1	100	0	100
Characteristics	Maximum size 4.8 mm		Maximum size 12.5 mm	
	Fineness modulus: 2.85		Fineness modulus: 3.73	

3 | EXPERIMENTAL PROCEDURES

3.1 | Crafting concrete mixtures

Distinct exposure classes were adopted when crafting the mixtures under the specifications of EN 1992-1 and EN 206, so that classes that endure effects from various damaging agents could be observed, which are listed as follows:

- Mixture 1: specified for X0 exposure class, regarding structures exposed to dry weathers.
- Mixture 2: Specified for XC2 exposure class, allusive to structures that undergo water forces.
- Mixture 3: specified for XD3 exposure class, concerning structures subjected to environments with salty fog.
- Mixture 4: specified for XA3 exposure class, namely structures within environments that pose chemical aggression.

Table 1 summarizes the characteristics of the mixtures. Portland cement with addition of 5% carbonate material was used as binding agent in this study. Figure 1 depicts the cement particle-size distribution.

The parameters of the cement evaluated are noteworthy, considering, for instance, the average diameter of particles of 16.77 μm, D10 of 5.34 μm, D50 of 15.21 μm, and D90 of 33.95 μm.

The fine aggregate was natural river quartz sand, while the coarse aggregate had basalt origin. The physical properties of the aggregates used are presented in Table 2.

A superplasticizer based on polycarboxylates was used to increase slump of the samples, which was fixed in 100 mm, for every water/cement ratio. The mixing was performed in a vertical axis mixer with mixing time of 16 minutes. The specimens were stored in a climate chamber with 23 ±2 °C and humidity of 100%.

The mixtures were crafted according to the characteristics stated above, with specimen dimensions of 100 x 200 mm for the compressive strength test at 28 days of cure and 5 × 20 mm for the mercury intrusion test, which were fragments from the specimens molded. For the 3D microtomography analysis, the sample presented approximate volume of 1 cm^3.
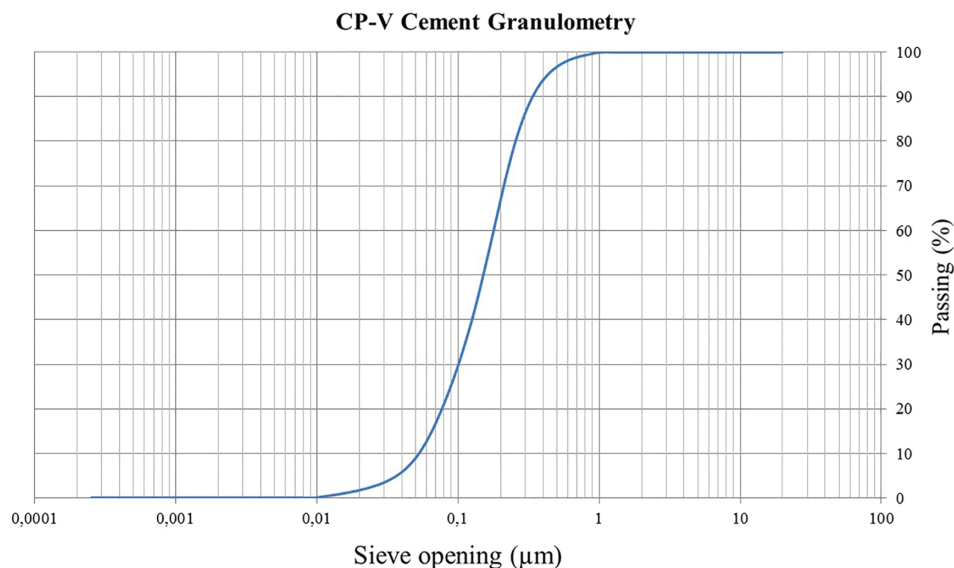

FIGURE 1 Composition characteristics of mixtures

3.2 | Mercury intrusion porosimetry test

The porosity of concretes was determined through the MIP test. The sample was dried in an oven until reaching constant mass. The apparatus used was Porosimetry model Pore Master 33, which quantifies the volume of pores from 200 to 0.0070 μm by applying variable pressures. The test was performed at 84 days, so that the compressive strength would be stabilized as well, and with the purpose of comparing the mixtures.

3.3 | 3D microtomography test

The 3D microtomography test for samples was conducted in an electrical characterization laboratory. A tomograph that makes X-ray images of samples with total volume of 1.0 cm^3 was used for such test. The sample underwent a pre-drying procedure and the test was performed at 28 days of cure. The images were generated by the CTPRO 3D software (Volume Graphics, Germany), which also made the volumetry, as shown in Figure 2. The Vg Studio Maxx software (Volume Graphics, Germany) was used in sequence, with the tools of Surface determination and Analysis. This software follows a color chart to evaluate voids of different sizes found in the volumetry.

4 | RESULTS AND DISCUSSION

4.1 | Compressive strength

Table 3 presents the compressive strength values of each of the four mixtures at 28 days. As noticed, the compressive strength values remained close to those specified by EN 1992-1, considering the exposure classes mentioned previously. Higher values of cement consumption, added to a reduction of the water/cement ratio led to an increase of compressive strength.

4.2 | Mercury intrusion porosimetry

Figure 3 depicts values for volume of mercury accumulated within the samples of mixtures, through which the highest
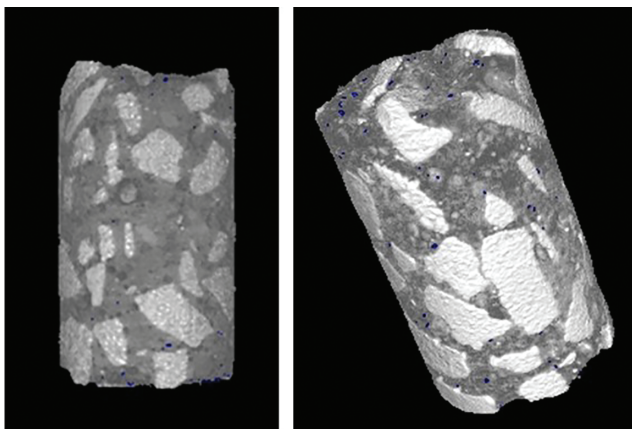

FIGURE 2 Volumetry made for the analysis of voids

TABLE 3 Compressive strength at 28 days

Mixture	Compressive strength (MPa) at 28 days	
	28 days	As per EN 1992-1
M1	23.8	25
M2	28.7	30
M3	34.4	35
M4	41.2	40

volume was achieved by M2. A relation between compressive strength and porosity was noted for the other mixtures, so M4 is characterized as the one with the least volume of mercury accumulated, indicating less pores. Analyzing the compositions that yielded the highest and the lowest volumes accumulated (M2 and M4, respectively), the volume of mercury for M4 was 11% smaller.

Figure 4 depicts the distribution of volumes with respect to the diameter of pores. Hence, the distribution of the volume of mercury intruded struck pores smaller than 0.1 μm. M2, whose behavior differed from the other samples, presented a peak of intrusion for pores with sizes 1 to 10 μm. It should be noted that this point of greater mercury penetration might have caused the difference of sample 2, considering both the distribution of pores and the total porosity presented in Figure 4. This point might also have been caused by a mistake in the composition of the original sample, from damages during consolidation, for example.

The results for M1, M3, and M4 are consistent with models proposed in other studies,[26] as porosity was inversely proportional to the samples' compressive strength. Total porosity has been known for being less related to compressive strength if compared to the influence exerted by pore size distribution, considering that this distribution varies with respect to the water/cement ratio and the paste's hydration degree.[30] The cement consumption also varied between these mixtures, so it might have influenced porosity.

Following a classification method proposed by Mehta and Monteiro,[1] it can be stated that the volume of mercury intruded struck pores with diameters between 10^{-7} and 10^{-3} m, which end up representing the physical phenomenon of capillary absorption.

4.3 | 3D microtomography

The images presented in Figure 5 were generated by processing the samples during the 3D microtomography test. These identify pores and their diameter, presented in scale, and yield the volumes with the respective calculation of voids within each specimen, as depicted in Figures 6 and 7.

Now, Figure 5 denotes a predominance of voids with volumes between 10 and 25 mm^3. Considering spherical volumes, the pores presented sizes by 10^{-3} m, in accordance with what had been assessed during the MIP test.
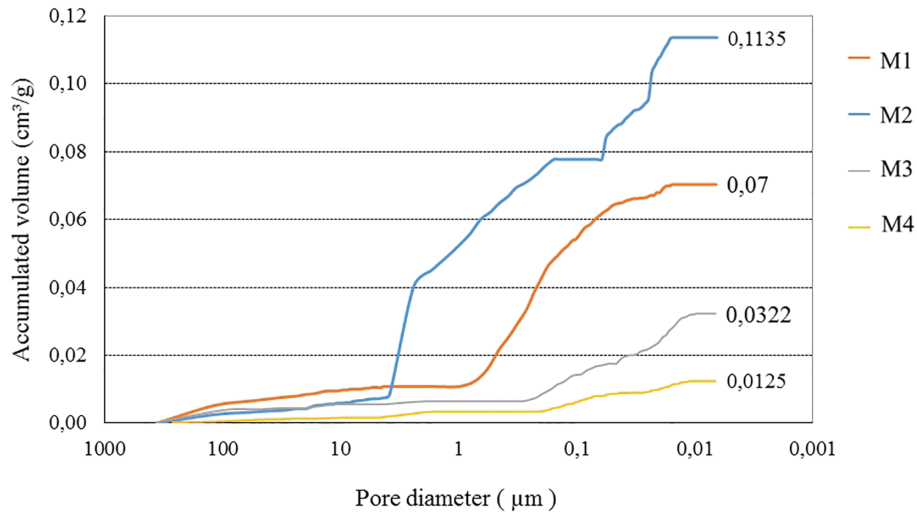
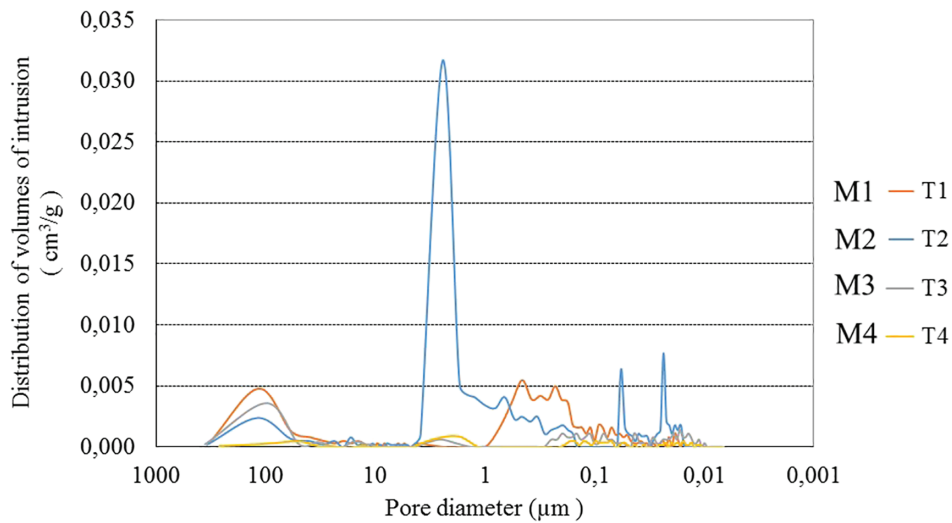**FIGURE 3**   Results for volumes of mercury accumulated within each sample

FIGURE 4   Volume distribution with respect to diameter of pores of each sample
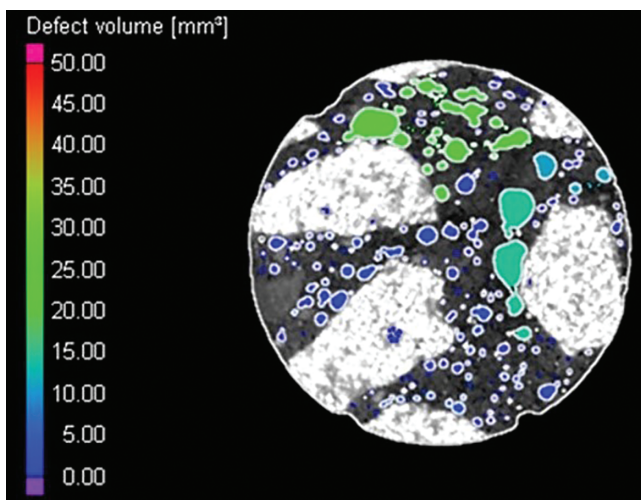

FIGURE 5   Void ratio identification

As checked in Figure 7, M1 had its pores distributed homogeneously, mainly because there was little concentration around the coarse aggregates. M2 displayed similar behavior, as neither samples yielded volumes above 35 mm^3.

Comparing Figures 6 and 7, less voids can be noted for M3 and M4, and the volumes of voids remained at the outer edge of the coarse aggregates. Table 4 presents the sequence of results, referring to the total percentage of voids measured by the software.

The difference between mixtures was greater for the 3D microtomography test than for the MIP test, varying proportionally to higher values of cement consumptions and lower water/cement ratio, while being inversely proportional to the mixtures' compressive strength. No outliers were spotted during this analysis.

Upon examining the compositions, it is noteworthy that the volume yielded by M4 was 27.5% lower than that of M1, whereas the percentages of reduction were 22.3% and 13% for M3 and M2, respectively.

Particularly in terms of voids index, the use of microtomography is recommended to distinguish materials whose
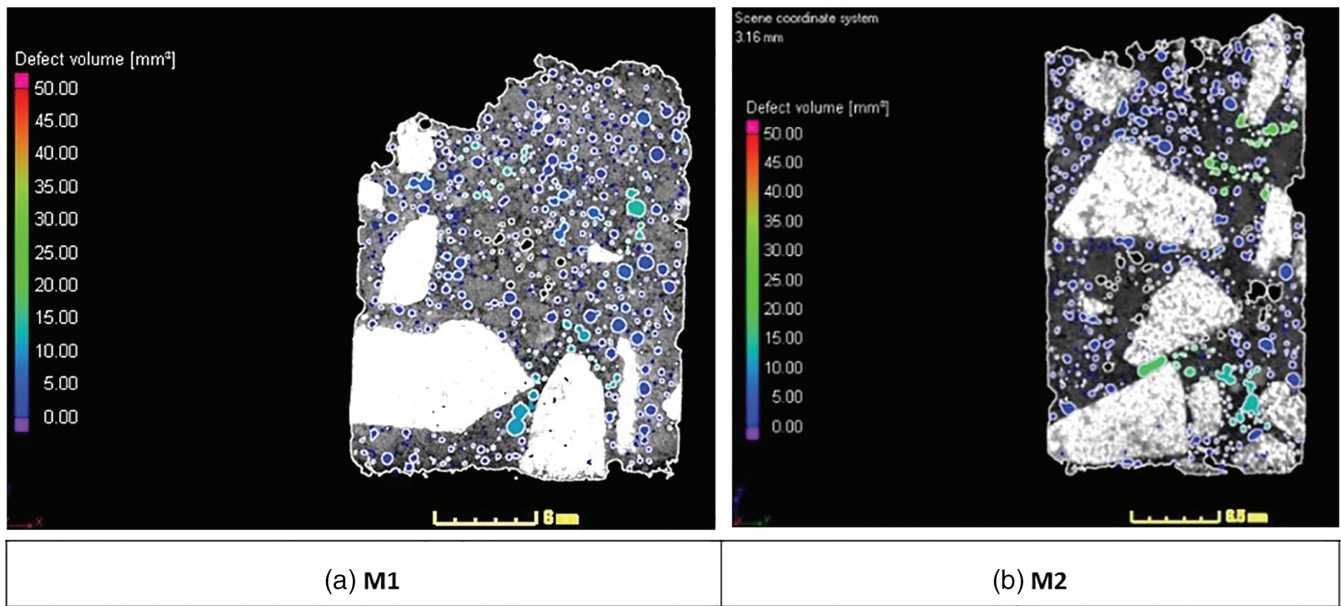
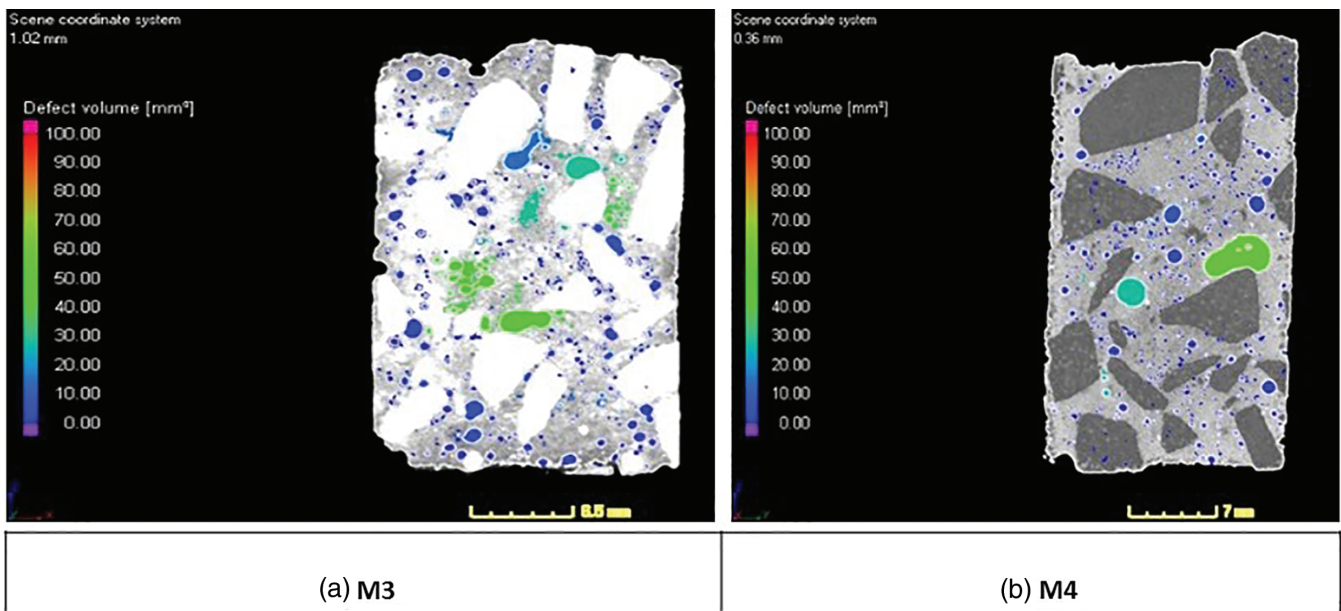FIGURE 6   Identification of voids contained by each composition

FIGURE 7   Identification of voids contained by each composition

TABLE 4   Void ratio of the mixtures

Mixture	M1	M2	M3	M4
Void ratio	12.39	10.78	9.62	8.98

specific gravity shows significant differences, as this is the procedure followed by the software for comparing specific gravity and quantifying different materials or voids.[31] It is difficult to analyze images from sample cuts, as is often confusion to identify its outlines and voids on its borders, what can impact the total volume observed, as Figure 8 shows. Such effect has already been identified on the border of images of concrete mixtures and turned out to be a likely spot of water accumulation during the molding process.[32]

4.4 | Comparative analysis

The relation presented in Figure 9 comes in handy for clarifying the comparative analysis between mixtures and the variables studied. It demonstrates that the mixture with the lowest compressive strength yielded the highest volume of voids for 3D microtomography, and the second highest for the porosimetry test. For the others, a linear relation was maintained between mixtures and measurements, comprising: as compressive strength increases, the volume of voids decreases for both methods of verification.

Taking into account the similarity between the tests performed with respect to identification of voids, Figure 10 proposes a relation between the mixtures' compressive strength and the tests for quantifying voids. Hence, both of the

FIGURE 8   Identification of voids contained by each composition

methods applied turned out to be strongly correlated to compressive strength, whereas 3D microtomography performed superiorly in the comparative analysis. The relation for both tests was obtained by means of a polynomial function. Lastly, it is noticeable that the void ratio results vary between methods, since the porosimetry test does not

identify pores that do are not interconnected, while the 3D microtomography method does.

5 | CONCLUSION

This paper development made it possible to observe the assertive nature of specifications set by technical standards, especially by EN 1992-1. The specification of the characteristics of cement consumption and water/cement ratio led to compressive strengths close to those required by this standard, aiming to ensure durability.

The advanced characterization tests showed a relation between the existence of voids and compressive strength, the exception being M2, which turned out to be an outlier compared with the other observations from the MIP test. An inversely proportional relation between compressive strength and volume of material intruded was observed for the other samples.

Given the characteristic size of pores, which left no signs that capillary absorption could occur, and considering that these samples might have pores aligned that allow deterioration agents to act, it was assessed within a scale of intensity that M1 is more likely to be attacked, and the likelihood reduces until M4, excluding the intrusion point of M2.
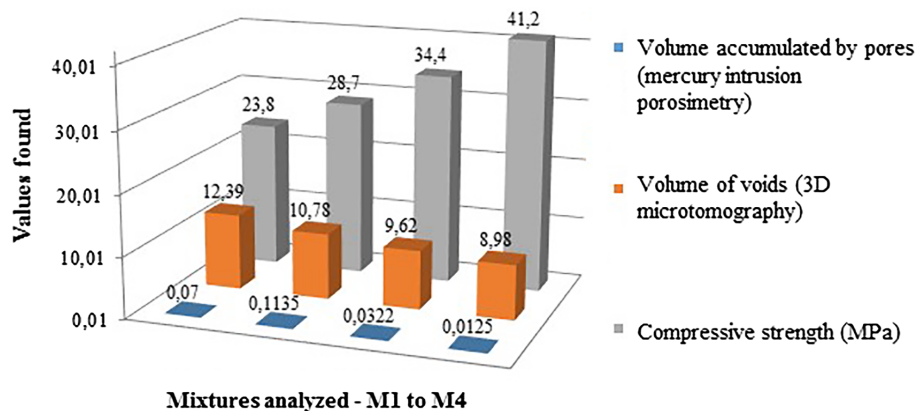

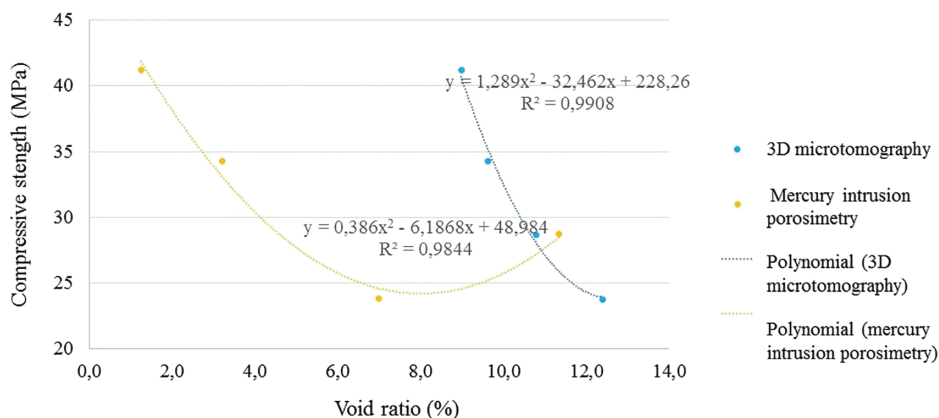**FIGURE 9**   Comparative analysis of variables studied

FIGURE 10   Relation between tests for quantifying voids and compressive strength

The 3D microtomography test was shown to be pertinent and effective for analyzing voids, as several authors had already reported, but attention should be drawn towards the bordering effect that may affect the images generated.

Overall, these diagnostic tests allow the characterization of structures regarding the existence of voids and may simultaneously determine the likelihood of the mixtures being damaged by these voids, consequently indicating how the durability of the material in use is going to behave.

It is also important to emphasize that the relation between tests of advanced diagnostic and compressive strength was determined in this study through simple low-cost methods, whereas without damaging the structure and with reduced scale samples, allowing for tests on structures that already were already built.

ACKNOWLEDGMENTS

ORCID

Bernardo Tutikian http://orcid.org/0000-0003-1319-0547

## REFERENCES

1. Mehta PK, Monteiro PJM. Concreto: Microestrutura, propriedades e materiais. 2nd ed. IBRACON: São Paulo, 2014.
2. Gjorv OE. Quality control and quality assurance for concrete durability. Key Eng Mater. 2016;711:76–83.
3. Bastidas-Arteaga E, Schoefs F, Stewart MG, Wang X. Influence of global warming on durability of corroding RC structures: A probabilistic approach. Eng Struct. 2013;51:259–266. https://doi.org/10.1016/j.engstruct.2013. 01.006.
4. American Concrete Institute. ACI 318–14: Building code requirements for structural concrete and commentary. Farmington Hills, MI: American Concrete Institute, 2014;p. 520.
5. Associação Brasileira de Normas Técnicas. NBR 6118 – Projeto de estruturas de concreto—Procedimento. Rio de Janeiro: Associação Brasileira de Normas Técnicas, 2014;p. 238.
6. Australian Standard. AS 3600: Concrete structures. Sydney: Standards Australia Limited, 2009.
7. Bureau of Indian Standards. IS 456: Plain and reinforced concrete – Code of practice. New Delhi: Bureau of Indian Standards, 2000.
8. European Committee for Standardization. EN 206-1: Concrete – Specification, performance, production and conformity. Brussels: European Committee for Standardization, 2013.
9. Muller HS, Haist M, Vogel M. Assessment of the sustainability potential of concrete and concrete structures considering their environmental impact, performance and lifetime. Constr Build Mater. 2014;67:321–337. https://doi.org/10.1016/j.conbuildmat.2014.01.039.
10. Flint MM, Baker JW, Billington SL. A modular framework for performance-based durability engineering: From exposure to impacts. Struct Saf. 2014;50:78–93. https://doi.org/10.1016/j.strusafe.2014.03.003.
11. Nganga G, Alexander M, Beushausen H. Practical implementation of the durability index performance based design approach. Constr Build Mater. 2013;45:251–261. https://doi.org/10.1016/j.conbuildmat.2013.03.069.
12. Chroma M, Rovnanikova P, Teply B, Strauss A. Effective water-cement ratio of concrete and its effect on the durability of concrete structures.

13. Proceedings of the International workshop on performance-based specification and control of concrete durability; 2014 Jun 11–13; Zagreb, Croatia; 2014.
13. Rabehi M, Mezghiche B, Guettala S. Correlation between initial absorption of the cover concrete, the compressive strength and carbonation depth. Constr Build Mater. 2013;45:123–129. https://doi.org/10.1016/j. conbuildmat.2013.03.074.
14. Ozturk AU, Onal O. Identification of water/cement ratio of cement pastes, basing on the microstructure image analysis data and using artificial neural network. KSCE J Civ Eng. 2013;17(4):763–768. https://doi.org/10.1007/s12205-013-0156-9.
15. Wassermann R, Katz A, Bentur A. Minimum cement content requirements: A must or a myth? Mater Struct. 2009;42(7):973–982. https://doi.org/10.1617/s11527-008-9436-0.
16. Choi YC, Kim J, Choi S. Mercury intrusion porosimetry characterization of micropore structures of high-strength cement pastes incorporating high volume ground granulated blast-furnace slag. Constr Build Mater. 2017;137:96–103. https://doi.org/10.1016/j.conbuildmat.2017.01.076.
17. Panesar DK, Francis J. Influence of limestone and slag on the pore structure of cement paste based on mercury intrusion porosimetry and water vapour sorption measurements. Constr Build Mater. 2014;52:52–58. https://doi.org/10.1016/j.conbuildmat.2013.11.022.
18. Reinke SK, Wilde F, Kozhar S, et al. Synchrotron X-ray microtomography reveals interior microstructure of multicomponent food materials such as chocolate. J Food Eng. 2016;174:37–46. https://doi.org/10.1016/j.jfoodeng.2015.11.012.
19. Hilloulin B, Legland JB, Lys E, et al. Monitoring of autogenous crack healing in cementitious materials by the nonlinear modulation of ultrasonic coda waves, 3D microscopy and X-ray microtomography. Constr Build Mater. 2016;123:143–152. https://doi.org/10.1016/j.conbuildmat.2016.06.138.
20. Duart MA. Estudo da microestrutura do concreto com adição de cinza de casca de arroz residual sem beneficiamento [unpublished dissertation]. Santa Maria: Civil Engineering Graduate Program, Universidade Federal de Santa Maria; 2008.
21. Ma H. Mercury intrusion porosimetry in concrete technology: Tips in measurement, pore structure parameter acquisition and application. J Porous Mat. 2014;21(2):207–215. https://doi.org/10.1007/s10934-013-9765-4.
22. Roziere E, Loukili A, Cussigh F. A performance based approach for durability of concrete exposed to carbonation. Constr Build Mater. 2009;23(1):190–199. https://doi.org/10.1016/j.conbuildmat.2008.01.006.
23. Pacheco F, Christ R, Gil AM, Tutikian BF. SEM and 3D microtomography application to investigate the distribution of fibers in advanced cementitious composites. Rev IBRACON Estrut Mater. 2016;9:824–841. https://doi.org/10.1590/s1983-41952016000600002.
24. Helene P. Contribuição ao Estudo da Corrosão em Armaduras de Concreto Armado [unpublished thesis]. São Paulo Polytechnic School of University of São Paulo; 1993, p. 248.
25. Lu S, Landis EN, Keane DT. X-ray microtomographic studies of pore structure and permeability in Portland cement concrete. Mater Struct. 2006;39(6):611–620. https://doi.org/10.1617/s11527-006-9099-7.
26. Abdin Y, Lomov SV, Jain A, Van Lenthe GH, Verpoest I. Geometrical characterization and micro-structural modeling of short steel fiber composites. Compos A: Appl Sci Manuf. 2014;67:171–180. https://doi.org/10.1016/j. compositesa.2014.08.025.
27. Gallucci E, Scrivener K, Groso A, Stampanoni M, Margaritondo G. 3D experimental investigation of the microstructure of cement pastes using synchrotron X-ray microtomography (µCT). Cem Concr Res. 2007;37:360–368. https://doi.org/10.1016/j.cemconres.2006.10.012.
28. Machado AC, Silva MA, Filho RDT, Pfeil MS, Lima I, Lopes RT. 3D investigation of steel fiber distribution in reinforced concrete by X-ray microtomography. Rev IBRACON Estrut Mater. 2015;8(5):707–720. https://doi.org/10.1590/S1983-41952015000500008.
29. du Plessis A, Olawuyi BJ, Boshoff WP, le Roux SG. Simple and fast porosity analysis of concrete using X-ray computed tomography. Mater Struct. 2014;49:553–562. https://doi.org/10.1617/s11527-014-0519-9.
30. Andrade JJO, Tutikian BF. Resistência mecânica do concreto. Ch. 17. ISAIA, Geraldo Cechella. Concreto: Ciência e Tecnologia. São Paulo: IBRACON, 2011; p. 615–651.

31. Temmyo T, Obara Y. Quantification of material constitution in concrete by X-ray CT method. Adv Comput Tomogr Geomater. 2013;17:140–147. https://doi.org/10.1002/9781118557723.ch17.

32. Leite MB, Monteiro PJM. Microstructural analysis of recycled concrete using X-ray microtomography. Cem Concr Res. 2016;81:38–38, 48. https://doi.org/10.1016/j.cemconres.2015.11.010.

AUTHOR BIOGRAPHIES
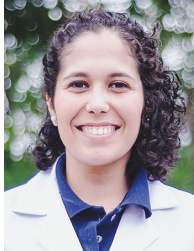
Fernanda Pacheco
Civil Engineering
Universidade do Vale do Rio dos Sinos
UNISINOS
itt Performance
fernandapache@unisinos.br

Rodrigo Périco de Souza
Universidade do Vale do Rio dos Sinos
UNISINOS
itt Performance
rperico@unisinos.br

Roberto Christ
Civil Engineering
Universidade do Vale do Rio dos Sinos
UNISINOS
itt Performance
rchrist@unisinos.br

Clarissa Argenti Rocha
Universidade do Vale do Rio dos Sinos
UNISINOS
itt Performance
clarirocha@unisinos.br

Luis Silva
Universidad de la Costa
CUC
lsilva8@cuc.edu.co

Bernardo Tutikian
Universidade do Vale do Rio dos Sinos
UNISINOS
itt Performance
bftutikian@unisinos.br